Iterative predictor-corrector method for extraction of the pair interaction from structural data for dense classical liquids

L. Reatto
Dipartimento di Fisica, Università degli Studi di Parma, I-43100 Parma, Italy

D. Levesque and J. J. Weis
Laboratoire de Physique Théorique et Hautes Energies, Université de Paris—Sud, 91405 Orsay, France
(Received 30 December 1985)

First, we demonstrate that careful simulations of fluids have enough accuracy that the resulting radial distribution function can be used to test inversion methods. Second, we introduce a method which allows extraction of the pair interaction starting from structural data for simple liquids even under triple-point condition. The method is an iterative predictor-corrector method in which the predictor is the modified hypernetted-chain equation and the corrector is simulation. We have verified the convergence of the method for the Lennard-Jones fluid and for a model potential for aluminum. We find that other methods of inversion give unreliable results. As a first application of our method we have inverted the experimental structural data of Na at 100 °C.

I. INTRODUCTION

Central to most present day theories of static properties of classical fluids is the study of the correlation functions,[1] in particular of the radial distribution function (RDF) $g(r)$. The basic problem is the determination of $g(r)$ given an interaction law between the particles. Usually this is assumed to have a spherical symmetry and a pairwise additive form for a one-component fluid of spherical particles. The method of integral equations for $g(r)$ and the perturbative approach have been developed for this direct problem and both approaches have reached a high degree of accuracy and flexibility, both with respect to the form of the two-body interaction $v(r)$ and to the thermodynamic state, low or high density, and low or high temperature.

A very significant aspect of the correlation function approach to the fluid state is that any such theory for $g(r)$ can be used in the reverse way, i.e., assuming known $g(r)$ one can solve the equation with respect to $v(r)$. This gives the possibility of obtaining information on the interatomic forces in the condensed phase starting from the measured structure factor $S(q)$ related to $g(r)$ by

$$S(q)=1+\rho\int d^3r\, e^{i\mathbf{q}\cdot\mathbf{r}}[g(r)-1]\ . \tag{1.1}$$

Since in a real system many-body forces are present, the extracted $v(r)$ will be an effective two-body interaction and it will in general be state dependent. Starting from the pioneering work of Johnson, Hutchinson, and March[2] this inverse problem has attracted much attention and over and over again experimental structure factors have been analyzed and effective interactions deduced.

Ideally one would like to have an inversion method whose accuracy does not depend on the detailed shape of $v(r)$, otherwise this could bias the result, in particular when we compare $v(r)$ of different substances. In addition, the method should have a comparable accuracy both at high and at low density. This is for two reasons. First, some of the most interesting systems, the liquid metals, are only found as a very dense fluid. The second reason is to be sure that any state dependence found in $v(r)$ reflects the presence of many-body forces and is not an artifact of the inversion method.

It turns out that this inverse problem is much more difficult than the direct one and this is easy to understand. At low density $g(r)$ is a faithful representation of $v(r)$ and, in fact, the low-density limit of $g(r)$ is $\exp[-v(r)/k_BT]$. On the contrary at high density, in the triple point region, $g(r)$ is very insensitive to the detailed shape of $v(r)$ and is mainly determined by the packing fraction of the system in terms of the excluded volume due to the repulsive part of $v(r)$. This, in fact, lies at the basis of the success of the perturbative approach to the liquid state starting from the hard-sphere system. The consequence of this in the inverse problem is that $v(r)$ has a very strong dependence on the precise value of $g(r)$ used as input. In addition, any small error of the theory in expressing $g(r)$ as a function of $v(r)$ gives an extremely amplified error on $v(r)$ when the same theory is used in the inverse problem.

Given this difficulty, it is important to figure out ways for testing any proposed inversion scheme. Simulation of model systems is ideally suited for this purpose. Starting from the $g(r)$ obtained from simulation one should apply the inversion method under a test and then directly compare the extracted $v(r)$ with the interaction used in the simulation. The first purpose of this paper is to determine if the accuracy of present-day typical simulation computation can be enough for the purpose of testing inversion methods.

The second purpose of our paper is to introduce an iterative predictor-corrector method for the solution of this inverse problem. In fact, we reach the conclusion that no theory of correlations so far introduced is accurate

enough for general use in the inversion problem. We overcome this difficulty by using a suitable theory of correlation, in our case a modified hypernetted-chain (MHNC) relation,[3] only as predictor of a trial pair interaction. Then a corrector stage follows in which simulation is used in order to obtain the "exact" RDF corresponding to the trial interaction. This cycle can be iterated until the trial interaction gives a RDF in agreement with the starting $g(r)$. This approach was introduced some time ago by one of us[4] in a formally similar problem in the theory of Bose quantum fluids and found[5] to converge. Here[6] we apply this iterative predictor-corrector method to the case of classical fluids. First we test the method for two models, the Lennard-Jones (LJ) fluid and a fluid of particles interacting with a model interaction suitable for liquid aluminum. The general scheme of our method is similar to one used by Schommers.[7] We differ in a substantial way from Schommers in the choice of the predictor. This is crucial and in fact we have tested Schommers's scheme in the case of the LJ fluid and we do

TABLE I. Tabulation of the following correlation functions: $g(r)$, $c(r)$, $E(r)$, and $S(q)$ for the Lennard-Jones fluid at $\rho\sigma^3=0.84$ and $k_BT/\varepsilon=0.75$ and with the potential cut off at $r_c=4\sigma$. Beyond this distance $g(r)$ is extended with the algorithm (2.10). To take into account the finite size in the computation of $E(r)$ from (2.6) we have used $\beta v(r)=\ln[\overline{\exp(-\beta v)}]$, where the average is over the grid size centered at r.

r/σ	$g(r)$	$c(r)$	$E(r)$	$q\sigma$	$S(q)$	r/σ	$g(r)$	$c(r)$	$E(r)$	$q\sigma$	$S(q)$
0.04	0.000	−35.512		0.31	0.041	1.38	0.764	0.627	−0.068	14.11	0.998
0.08	0.000	−35.532		0.61	0.041	1.40	0.720	0.589	−0.075	14.42	0.933
0.12	0.000	−33.116		0.92	0.041	1.42	0.684	0.551	−0.085	14.73	0.884
0.16	0.000	−31.455		1.23	0.040	1.44	0.653	0.511	−0.100	15.03	0.853
0.20	0.000	−29.687		1.53	0.040	1.46	0.630	0.475	−0.112	15.34	0.840
0.24	0.000	−27.892		1.84	0.041	1.48	0.615	0.442	−0.119	15.65	0.841
0.28	0.000	−26.107		2.15	0.043	1.50	0.602	0.406	−0.131	15.95	0.856
0.32	0.000	−24.350		2.45	0.045	1.52	0.593	0.371	−0.143	16.26	0.883
0.36	0.000	−22.628		2.76	0.049	1.56	0.592	0.306	−0.155	16.57	0.920
0.40	0.000	−20.944		3.07	0.055	1.60	0.605	0.248	−0.159	16.87	0.963
0.44	0.000	−19.302		3.37	0.064	1.64	0.633	0.197	−0.154	17.18	1.007
0.48	0.000	−17.706		3.68	0.076	1.68	0.680	0.161	−0.131	17.49	1.047
0.52	0.000	−16.160		3.99	0.093	1.72	0.744	0.140	−0.098	17.79	1.080
0.56	0.000	−14.671		4.30	0.118	1.76	0.817	0.129	−0.064	18.10	1.101
0.60	0.000	−13.242		4.60	0.155	1.80	0.904	0.132	−0.025	18.41	1.109
0.64	0.000	−11.880		4.91	0.213	1.84	0.991	0.136	−0.002	18.71	1.104
0.68	0.000	−10.588		5.22	0.309	1.88	1.071	0.135	−0.014	19.02	1.088
0.72	0.000	−9.367		5.52	0.477	1.92	1.140	0.124	−0.011	19.33	1.066
0.76	0.000	−8.219		5.83	0.788	1.96	1.198	0.105	−0.005	19.63	1.041
0.80	0.000	−7.144		6.14	1.356	2.00	1.239	0.076	−0.031	19.94	1.015
0.84	0.000	−6.140		6.44	2.190	2.04	1.265	0.047	−0.056	20.25	0.990
0.88	0.000	−5.209		6.75	2.678	2.08	1.275	0.029	−0.068	20.56	0.967
0.92	0.013	−4.338	−2.738	7.06	2.283	2.12	1.258	0.017	−0.070	20.86	0.950
0.94	0.078	−3.872	−2.425	7.36	1.652	2.16	1.221	0.015	−0.059	21.17	0.939
0.96	0.279	−3.291	−2.148	7.67	1.202	2.20	1.166	0.017	−0.042	21.48	0.934
0.98	0.690	−2.519	−1.886	7.98	0.930	2.24	1.103	0.020	−0.026	21.78	0.935
1.00	1.286	−1.584	−1.645	8.28	0.770	2.28	1.036	0.020	−0.018	22.09	0.943
1.02	1.928	−0.624	−1.428	8.59	0.678	2.32	0.974	0.018	−0.016	22.40	0.955
1.04	2.468	0.212	−1.229	8.90	0.628	2.36	0.927	0.020	−0.014	22.70	0.971
1.06	2.813	0.831	−1.047	9.20	0.608	2.40	0.884	0.012	−0.023	23.01	0.989
1.08	2.945	1.215	−0.883	9.51	0.612	2.44	0.855	0.005	−0.031	23.32	1.007
1.10	2.906	1.406	−0.737	9.82	0.636	2.48	0.842	0.001	−0.035	23.62	1.023
1.12	2.742	1.451	−0.610	10.12	0.680	2.52	0.837	−0.005	−0.041	23.93	1.035
1.14	2.513	1.410	−0.501	10.43	0.745	2.56	0.843	−0.010	−0.043	24.24	1.042
1.16	2.269	1.333	−0.405	10.74	0.830	2.60	0.859	−0.014	−0.043	24.54	1.046
1.18	2.031	1.244	−0.322	11.04	0.933	2.64	0.885	−0.014	−0.037	24.85	1.044
1.20	1.808	1.150	−0.253	11.35	1.045	2.68	0.917	−0.012	−0.030	25.16	1.038
1.22	1.604	1.059	−0.200	11.66	1.147	2.72	0.951	−0.012	−0.026	25.46	1.028
1.24	1.431	0.982	−0.155	11.97	1.222	2.76	0.990	−0.007	−0.019	25.77	1.017
1.26	1.282	0.914	−0.120	12.27	1.262	2.80	1.024	−0.005	−0.016	26.08	1.006
1.28	1.152	0.851	−0.097	12.58	1.268	2.84	1.053	−0.003	−0.015	26.38	0.995
1.30	1.042	0.795	−0.083	12.89	1.249	2.88	1.077	−0.002	−0.014	26.69	0.986
1.32	0.950	0.745	−0.074	13.19	1.208	2.92	1.091	−0.004	−0.016	27.00	0.978
1.34	0.875	0.703	−0.069	13.50	1.147	2.96	1.097	−0.007	−0.019	27.30	0.973
1.36	0.815	0.665	−0.066	13.81	1.073	3.00	1.096	−0.008	−0.020	27.61	0.971

TABLE II. The same as for Table I for the model Al potential with $r_c = 2.04 r_0$ at $\rho = 0.0527$ atoms/Å^3 and $T = 1051$ K ($r_0 = 4.234$ Å, $q_0 = r_0^{-1}$).

r/r_0	$g(r)$	$c(r)$	$E(r)$	βv_{Al}	q/q_0	$S(q)$
0.04	0.000	−38.547			0.80	0.020
0.08	0.000	−35.971			1.60	0.022
0.12	0.000	−32.768			2.40	0.025
0.16	0.000	−29.542			3.20	0.030
0.20	0.000	−26.494			4.00	0.036
0.24	0.000	−23.646			4.80	0.045
0.28	0.000	−20.979			5.60	0.060
0.32	0.000	−18.475			6.40	0.085
0.36	0.000	−16.125			7.20	0.128
0.40	0.000	−13.922			8.00	0.204
0.44	0.000	−11.855			8.80	0.361
0.48	0.000	−9.911			9.60	0.719
0.52	0.001	−8.090			10.40	1.462
0.56	0.149	−6.273	−1.445	5.881	11.20	2.237
0.58	0.588	−5.070	−1.420	3.769	11.60	2.314
0.60	1.422	−3.529	−1.165	2.434	12.00	2.157
0.62	2.375	−1.931	−0.927	1.514	12.40	1.859
0.64	2.983	−0.744	−0.689	0.946	12.80	1.520
0.66	3.033	−0.182	−0.481	0.625	13.20	1.214
0.68	2.677	−0.093	−0.315	0.470	13.60	0.974
0.70	2.173	−0.215	−0.191	0.420	14.00	0.801
0.72	1.695	−0.368	−0.109	0.427	14.40	0.684
0.74	1.317	−0.475	−0.058	0.458	14.80	0.610
0.76	1.044	−0.523	−0.033	0.491	15.20	0.568
0.78	0.857	−0.526	−0.027	0.511	15.60	0.552
0.80	0.733	−0.503	−0.035	0.512	16.00	0.555
0.82	0.654	−0.465	−0.053	0.491	16.40	0.576
0.84	0.607	−0.421	−0.077	0.450	16.80	0.611
0.86	0.584	−0.376	−0.105	0.393	17.20	0.660
0.88	0.578	−0.332	−0.135	0.324	17.60	0.722
0.90	0.586	−0.289	−0.162	0.248	18.00	0.796
0.92	0.605	−0.250	−0.186	0.171	18.40	0.883
0.94	0.633	−0.213	−0.205	0.098	18.80	0.980
0.96	0.670	−0.176	−0.215	0.032	19.20	1.084
1.00	0.765	−0.102	−0.202	−0.067	20.00	1.260
1.04	0.889	−0.025	−0.145	−0.114	20.80	1.318
1.08	1.023	0.041	−0.073	−0.114	21.60	1.264
1.12	1.122	0.054	−0.034	−0.081	22.40	1.170
1.16	1.168	−0.001	−0.047	−0.033	23.20	1.063
1.20	1.186	−0.082	−0.085	0.012	24.00	0.955
1.24	1.197	−0.125	−0.098	0.044	24.80	0.871
1.28	1.173	−0.117	−0.074	0.056	25.60	0.827
1.32	1.094	−0.087	−0.041	0.050	26.40	0.826
1.36	0.992	−0.059	−0.028	0.031	27.20	0.865
1.40	0.910	−0.041	−0.039	0.007	28.00	0.934
1.44	0.869	−0.031	−0.055	−0.015	28.80	1.018
1.48	0.869	−0.023	−0.060	−0.028	29.60	1.089
1.52	0.895	−0.019	−0.056	−0.031	30.40	1.122
1.56	0.938	−0.017	−0.045	−0.025	31.20	1.115
1.60	0.984	−0.021	−0.034	−0.013	32.00	1.082
1.64	1.022	−0.029	−0.028	0.001	32.80	1.038
1.68	1.047	−0.037	−0.026	0.012	33.60	0.995
1.72	1.056	−0.044	−0.027	0.018	34.40	0.960
1.76	1.053	−0.043	−0.026	0.018	35.20	0.938
1.80	1.041	−0.036	−0.025	0.013	36.00	0.931

not find convergence to the correct answer. On the contrary, with our MHNC predictor we find the correct answer with high precision.

Having proved that our predictor-corrector method can be used to deduce the pair interaction with high accuracy, we apply the method to the experimental data for Na at 100 °C.

The contents of the paper are as follows. In Sec. II we study whether simulation data can be accurate enough in order to test inversion procedures and in addition test the MHNC procedure. In Sec. III we discuss predictor-corrector methods. In Sec. IV both our predictor-corrector method and Schommers's method are tested in the case of the LJ fluid. In Sec. V we apply our method to the model Al problem. In Sec. VI we discuss the applicability of our method to invert experimental data and as an example in Sec. VII we invert the experimental data for Na. Section VIII contains a discussion of our results and the conclusions. In Tables I and II we tabulate some of the correlation functions for the LJ fluid and for the model Al fluid.

II. SIMULATION AND THEORIES OF FLUID FOR THE INVERSE PROBLEM

We consider a one-component fluid of spherical particles interacting via a pair interaction

$$V=\frac{1}{2}\sum_{\substack{i,j\\ i\neq j}} v(r_{ij}) . \tag{2.1}$$

Standard integral equations[1] for the RDF $g(r)$ like the Percus-Yevick (PY) and the hypernetted chain (HNC) can be easily used in the inverse problem. For instance, the HNC closure

$$c(r)=-\beta v(r)+g(r)-1-\ln[g(r)] ,$$

where $\beta=(k_B T)^{-1}$, for the Ornstein-Zernike (OZ) direct correlation function $c(r)$ immediately gives the inversion formula

$$\beta v_{\mathrm{HNC}}(r)=g(r)-1-c(r)-\ln[g(r)] \tag{2.2}$$

if $g(r)$ of the system is known. $c(r)$ is related to $g(r)$ by the OZ relation

$$g(r)-1=c(r)+\rho\int d^3r' c(r')[g(|\mathbf{r}-\mathbf{r}'|)-1] , \tag{2.3}$$

so that it is given explicitly in terms of the structure factor $S(q)$ by

$$c(r)=\frac{1}{\rho(2\pi)^3}\int d^3q\left[1-\frac{1}{S(q)}\right]e^{-i\mathbf{q}\cdot\mathbf{r}} . \tag{2.4}$$

In a similar way the PY closure leads to the inversion formula

$$\beta v_{\mathrm{PY}}(r)=\ln[1-c(r)/g(r)] . \tag{2.5}$$

Both the PY and the HNC equations are not very accurate for fluids at high density so that also the inversion formulas (2.2) and (2.5) are not expected to be accurate. Many computations[8-10] have, in fact, verified this. Mixed integral equations between PY and HNC have been introduced and also used as an inversion procedure.[10,11] This approach suffers from the difficulty that the equations contain free parameters which can be determined by use of additional information on the properties of the system. For instance, the equation used by Brennan *et al.*[11] contains two parameters and these are fixed by two thermodynamic constraints, the value of the pressure and that of the internal energy. The presence of state-dependent interactions and of many-body forces in a real system makes ambiguous the use of similar constraints, in particular in the case of liquid metals when, in fact, more elaborate constraints[12] have been used.

Recently[3] the accuracy of the integral equation approach has been greatly improved, elaborating on the notion of a reference fluid first established with the perturbative approach of liquids. Starting from the insensitivity of $g(r)$ on the detailed shape of $v(r)$ under triple-point conditions, the perturbative approach obtains $g(r)$ and the thermodynamic properties of the system by an expansion around the values of a suitable reference fluid, usually the hard-sphere fluid. With the MHNC equation one starts with the formally exact relation

$$g(r)=\exp[-\beta v(r)+g(r)-1-c(r)+E(r/v)] \tag{2.6}$$

obtained from a resummation of the cluster expansion of $g(r)$. $E(r/v)$, the so-called bridge function, is the sum of the elementary diagrams, an infinite series of diagrams in terms of $h=g-1$ bonds. From the observation that $E(r/v)$ has a dependence on the shape of $v(r)$ even smaller than the one of $g(r)$, MHNC consists in approximating $E(r/v)$ in (2.6) with the bridge function $E_{\mathrm{HS}}(r,\eta)$ of hard spheres. The bridge function of hard spheres depends on only one parameter, the packing fraction $\eta=\pi\rho d^3/6$, where ρ is the number density and d the diameter. The variational principle for the free energy gives the equation[13]

$$\int d^3r[g(r)-g_{\mathrm{HS}}(r,\eta)]dE_{\mathrm{HS}}(r,\eta)/d\eta=0 , \tag{2.7}$$

which determines η uniquely if g_{HS} and E_{HS} are assumed to be known.

MHNC used in the inversion procedure leads immediately to the expression

$$\beta v_{\mathrm{MHNC}}=g(r)-1-c(r)-\ln[g(r)]+E_{\mathrm{HS}}(r,\eta) . \tag{2.8}$$

Since MHNC used in the direct problem gives excellent results for $g(r)$ when compared with simulation results for a number of pair interactions, it might be anticipated that (2.8) should give an accurate inversion of $g(r)$.

In fact, the MHNC relation has already been used[14,15] to extract the pair interaction from experimental data and claimed[14] to be accurate. Here we test this method starting from $g(r)$ obtained from simulation.

First we consider the Lennard-Jones potential

$$v_{\mathrm{LJ}}(r)=-4\varepsilon[(\sigma/r)^6-(\sigma/r)^{12}] \tag{2.9}$$

under triple-point conditions, $\rho^*=\rho\sigma^3=0.84$ and $T^*=k_B T/\varepsilon=0.75$. We have generated by molecular dynamics $g(r)$ for a system of 864 particles with three long runs. Two runs are of 16 800 integration steps and v_{LJ} is truncated at $r_c=2.5\sigma$. One run is of 6800 integration steps with $r_c=4\sigma$. In both cases $g(r)$ is computed up

to the respective r_c. In order to obtain $c(r)$ from (2.4) the structure factor $S(k)$ has been computed by first extending $g(r)$ for $r>r_a$ with Verlet's algorithm:[8] the OZ relation (2.3) has been solved with the condition

$$g(r)=g_{\rm sim}(r), \quad r<r_a \tag{2.10a}$$

where $g_{\rm sim}(r)$ is the raw simulation result and

$$c(r)=-\beta v(r), \quad r>r_a \ . \tag{2.10b}$$

For the particular case where r_a is chosen equal to r_c, (2.10b) reduces to $c(r)=0$ for $r>r_a$. Then $\beta v_{\rm MHNC}$ is obtained from (2.8) with η determined by solving (2.7). We find that the extracted interaction is not satisfactory as can be seen in Fig. 1(a); the minimum of $\beta v_{\rm LJ}$ is underestimated by $\sim 20\%$ and a spurious structure appears at $r\sim 1.7\sigma$. Before accepting this negative result we must critically examine if the input data $g_{\rm sim}$ are adequate for our purpose. In fact, there are many possible sources of errors. First, $g(r)$ is known over a finite range and the data must be extended to large distance. The method (2.10) is only approximate and this introduces an error in $c(r)$ and thus in $\beta v_{\rm MHNC}$ also for $r<r_c$. We have extended the results with cutoff $r_c=4\sigma$ for two values of $r_a=4\sigma$ and 2.5σ. The change in $\beta v_{\rm MHNC}$ is rather small and, in particular, negligible compared with the difference between $\beta v_{\rm MHNC}$ and $\beta v_{\rm LJ}$. Use of PY or HNC closures for c (2.10b) leads to a similar conclusion so that we believe that the extension scheme in itself is quite accurate even for cutoffs as small as 2.5σ.

Despite this satisfactory result we want to stress that the extension procedure (2.10) may not be easy to use near triple-point conditions, where the convergence of the iterative solution of the OZ equation is slow and quite sensitive to statistical noise in the $g(r)$.

A second source of error is the use of an approximate $E_{\rm HS}$ and $g_{\rm HS}$ in (2.7) and (2.8). We have used for $g_{\rm HS}$ the Verlet-Weis[16] parameterization $g_{\rm HS}^{\rm VW}$ of simulation data for hard spheres and this is not exact. Therefore, also $E_{\rm HS}$ obtained from

$$E_{\rm HS}^{\rm VW}(r)=c_{\rm HS}^{\rm VW}(r)-g_{\rm HS}^{\rm VW}(r)+1+\ln y_{\rm HS}^{\rm VW}(r) \ ,$$
$$y(r)=e^{\beta v(r)}g(r) \tag{2.11}$$

is only approximate. Again we estimate that this source of error is minor. In fact, we have obtained $\beta v_{\rm MHNC}$ also starting from the same $g(r)$ but using for $E_{\rm HS}$ and $g_{\rm HS}$ the PY approximation. Equation (2.7) gives now a slightly different value for η and this to a large extent compensates the difference between $E_{\rm HS}$ given by the two approximations for the same η. As a result, $\beta v_{\rm MHNC}$ shows only modest changes with respect to the result shown in Fig. 1(a).

A further problem derives from the statistical noise that affects $g_{\rm sim}(r)$ due to the statistical nature of the simulation methods. Using separately the two $g_{\rm sim}(r)$ obtained from the long runs with $r_c=2.5\sigma$ we have extracted two $\beta v_{\rm MHNC}$ and in Fig. 1(b) we plot the corresponding deviation $\Delta\beta v_{\rm MHNC}$. Even if MHNC does not accurately give the interaction, this deviation $\Delta\beta v_{\rm MHNC}$ can be taken as a very accurate representation of the intrinsic effect of the noise in $g_{\rm sim}(r)$. In fact, the error introduced by

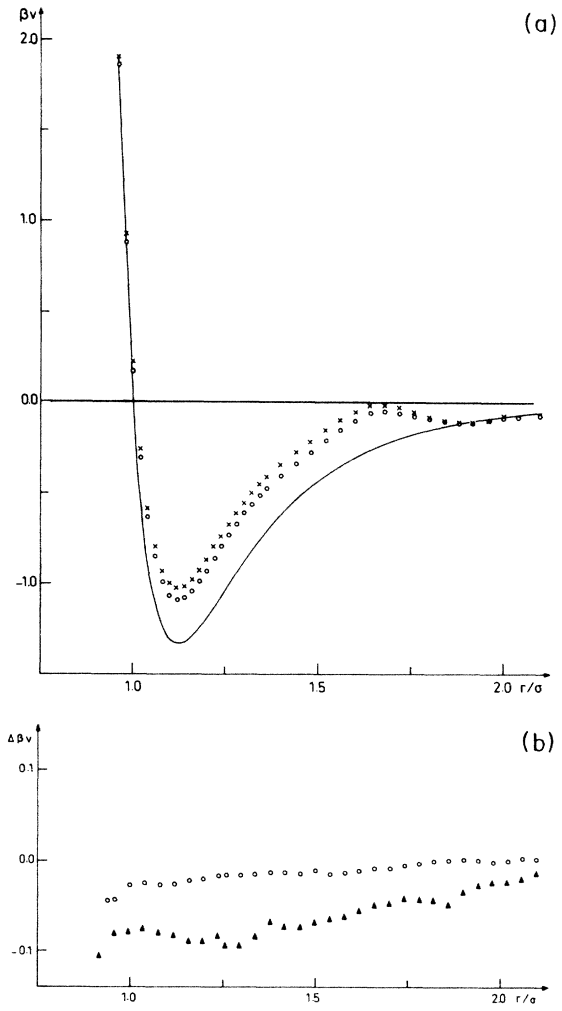

FIG. 1. (a) The potential $\beta v_{\rm MHNC}$ extracted from the computer simulated $g(r)$ of a Lennard-Jones system at $\rho^*=0.84$ and $T^*=0.75$ by means of the MHNC equation (2.8). The open circles and the crosses denote results corresponding to $g(r)$ obtained with potential cutoffs $r_c=4\sigma$ and 2.5σ, respectively, and extended beyond $r_a=r_c$ via Eq. (2.10). The solid line represents the exact Lennard-Jones potential. (b) Effect of the statistical noise in the computer simulated $g(r)$ on the extracted potential $\beta v_{\rm MHNC}$. The open circles represent the difference between the extracted pair potentials corresponding to two independent molecular-dynamics runs of 16 800 time steps each for a Lennard-Jones system with potential cutoff 2.5σ at $\rho^*=0.84$ and $T^*=0.75$, the triangles represent the difference between the extracted potentials from a run of 16 800 time steps and from $g(r)$ obtained by averaging over a block of 1600 time steps in the same run.

MHNC due to the approximation of the exact but unknown $E(r/v)$ with $E_{\rm HS}(r)$ will cancel out to a large extent when we take the difference between the two extracted potentials. From the result in Fig. 1(b) we conclude that the statistical noise of simulation for long runs is very small, giving an uncertainty in the extracted βv which typically is below ± 0.02, becoming somewhat larger in the core region but below the 1% level. However, the error becomes much larger for short runs. As an

example, in Fig. 1(b) we plot also the deviation $\Delta\beta v_{\mathrm{MHNC}}$ between the extracted potential from one of the long runs and from $g(r)$ obtained by averaging over a block of 1600 time steps in the same run.

As a second test of inversion procedures we have considered a model potential[17] v_{Al} for aluminum. We have chosen this potential on one hand because it has the typical oscillations of the effective ion-ion interaction of liquid metals. In addition, it appeared *a priori* very difficult to reproduce because of several unusual features: it has a well-defined structure also at short distance where βv is positive (see Fig. 2); the subsequent oscillations have a rather small amplitude and the first peak of $g(r)$ for the Al density ($\rho=0.0527$ atom/Å^3) is at $r^*\approx 0.66$ ($r^*=r/r_0$ with $r_0=4.234$ Å), where βv is still well positive. In addition, the system is very incompressible at the temperature we consider, $T=1051$ K, with $S(q=0)\approx 0.02$, which is about half of the value of the LJ at the triple point. This means that the screening of the weak features of βv_{Al} by the repulsive part of the interaction is even more pronounced than in the case of the LJ fluid.

We have performed with v_{Al} several Monte Carlo runs for 864 particles with a cutoff $r_c^*=2.04$. Usually, $g(r)$ has been computed up to r_c^* but in one run it has been computed up to 2.5. In Fig. 2 we plot the extracted βv_{MHNC} obtained from $g(r)$ of a run of 8400 moves/particle. MHNC gives the basic features of βv_{Al}, in particular the positions of some of the extrema of v_{Al}; however, the values at the extrema are given with rather large errors. In order to test if the cutoff distance $r_c^*=2.04$ is large enough such that the results are not affected by the extension procedure (2.10), we have extended the $g(r)$ of the run with the larger cutoff starting both from $r_a^*=2.5$ and also from 2.04. In Table III we give positions and values of the extracted βv_{MHNC} in a number of cases. Again the conclusion is that simulation can give $g(r)$ with enough accuracy to test inversion procedures. An additional conclusion is that MHNC is not accurate enough to represent an inversion procedure of quantitative

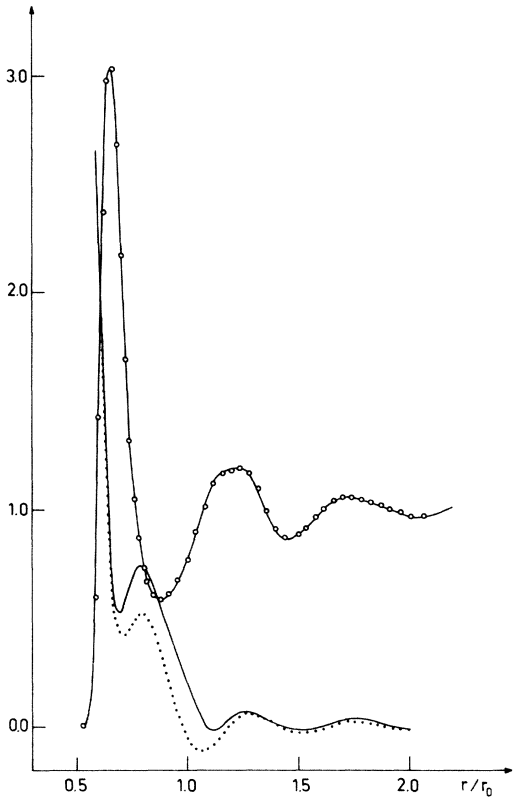

FIG. 2. Potential βv_{MHNC} (solid line) extracted from the MHNC equation (2.8) for an aluminumlike model system. The dots represent the aluminum model potential and the open circles the corresponding RDF obtained by a Monte Carlo simulation for $\rho=0.0527$ atom/Å^3 and $T^*=1051$ K.

value. Notice that this conclusion does not depend on the criterion (2.7) for the choice of the hard-sphere diameter. For instance, in the case of the LJ system no choice of η is able to eliminate the spurious shoulder at $r^*\approx 1.7$ and the value of η can be chosen so that βv_{MHNC} has the

TABLE III. Test of the inversion procedure (3.2) for a model aluminum potential. The first line gives the positions (in units of $r_0=4.234$ Å) and values of the minima (m_i,βv_{mi}) and maxima (M_i,βv_{Mi}) of the exact Al potential (Ref. 17). The four next lines compare the initial potential βv_0 obtained from the MHNC equation (2.8) for different Monte Carlo runs and different ways of extension of the RDF. *A*: run of 10^6 configurations, r_c (potential cutoff) is $2.08r_0$, r_a [cutoff used in the extension procedure (2.10)] is $2.08r_0$. *B*: run of 10^6 configurations, $r_c=2.08r_0$, $r_a=2.50r_0$ (in this run the RDF has been calculated up to $2.5r_0$). *C*: same run as *B* but $r_a=2.08r_0$. *D*: run of 8400 moves/particles, $r_c=r_a=2.04r_0$. The next lines give the potentials extracted after the first, fourth, sixth, and eighth iterations and the last line ($\beta\bar{v}_{4-8}$) the average potential from iterations 4–8.

	m_1	βv_{m_1}	M_1	βv_{M_1}	m_2	βv_{m_2}	M_2	βv_{M_2}	m_3	βv_{m_3}
Exact	0.71	0.420	0.79	0.512	1.06	−0.119	1.29	0.056	1.51	−0.031
$\beta v_0 A$	0.69	0.472	0.79	0.673	1.12	−0.092	1.28	−0.0008	1.47	−0.061
$\beta v_0 B$	0.69	0.485	0.79	0.675	1.12	−0.095	1.27	−0.020	1.49	−0.117
$\beta v_0 C$	0.69	0.487	0.79	0.673	1.12	−0.106	1.27	−0.027	1.49	−0.111
$\beta v_0 D$	0.69	0.525	0.79	0.743	1.12	−0.025	1.28	0.060	1.50	−0.015
βv_1	0.71	0.535	0.79	0.58	1.06	−0.084	1.28	0.065	1.50	−0.011
βv_4	0.71	0.38	0.79	0.50	1.06	−0.12	1.28	0.062	1.54	−0.006
βv_6	0.71	0.44	0.79	0.54	1.06	−0.07	1.28	0.095	1.50	−0.016
βv_8	0.71	0.36	0.79	0.49	1.06	−0.09	1.28	0.10	1.50	+0.017
$\beta\bar{v}_{4-8}$	0.71	0.39	0.79	0.50	1.06	−0.10	1.28	0.08	1.52	+0.002

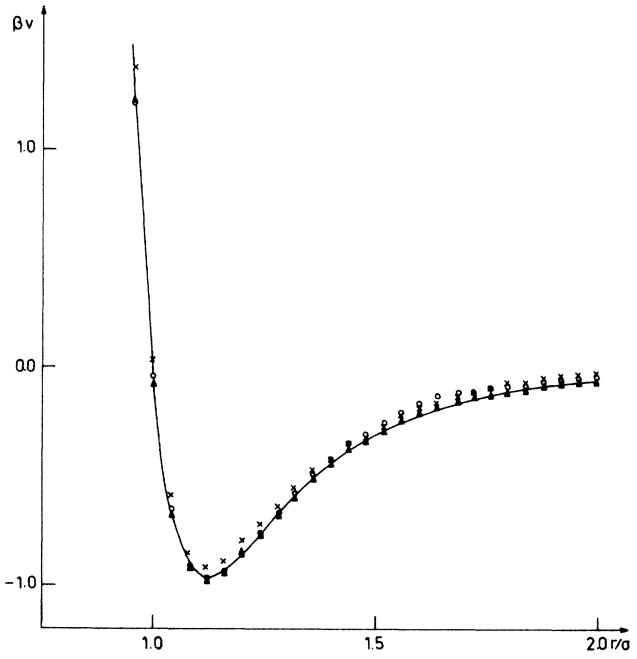

FIG. 3. Pair potential extracted from the RDF of a Lennard-Jones system at $\rho^*=0.65$ and $T^*=1.036$. The open circles represent βv_{MHNC} used as initial potential in the iterative predictor-corrector scheme (3.2). The crosses and the solid triangles represent the potentials extracted after the first and the last (fifth) iteration, respectively. The solid line represents the exact Lennard-Jones potential (divided by k_BT).

correct value at the minimum but in this case the potential is strongly underestimated in the core region.

Our conclusions regarding MHNC as an inversion procedure refer to triple-point conditions. At smaller density this procedure becomes rather accurate. As an example, see Fig. 3 where βv_{MHNC} is shown for the LJ system at $\rho\sigma^3=0.65$ and $k_BT/\varepsilon=1.036$.

For reference purposes we tabulate in Tables I and II some correlation functions for the LJ fluid under triple-point condition and for the Al model potential. We give $g(r)$ and $S(q)$, the direct correlation function $c(r)$, and the bridge function $E(r)$.

III. PREDICTOR-CORRECTOR METHODS FOR INVERSION

Suppose that using MHNC we have obtained a pair interaction v_{MHNC} starting from a given RDF $g(r)$. As shown in Sec. II, v_{MHNC} differs from the true $v(r)$ because of the approximation inherent to MHNC. We can improve on this if we consider $v_{\mathrm{MHNC}}(r)$ only as an initial estimate, which we call $v_0(r)$, of the exact $v(r)$. In fact, given $v_0(r)$ we can compute "exactly" the corresponding RDF, which we call $g_0(r)$, by use of simulation methods. If the predictor, MHNC in our case, were exact we should find $g_0(r)=g(r)$ within the statistical noise. This will not be so because $v_0(r)$ differs from $v(r)$ but we can use the difference $g(r)-g_0(r)$ to correct our first estimate. In fact, for the system $v_0(r)$ we can construct its bridge function

$$\begin{aligned} E(r/v_0)&=-g_0(r)+1+c_0(r)+\ln[y_0(r)]\ , \\ y_0(r)&=e^{\beta v_0(r)}g_0(r)\ , \end{aligned} \tag{3.1}$$

where $c_0(r)$ is the direct correlation function corresponding to $g_0(r)$. Since $v_0(r)$ will be, in any case, closer to $v(r)$ than the hard-sphere potential, it must be expected that we will get an improved estimate of the interaction $v(r)$ if we approximate the unknown $E(r/v)$ with $E(r/v_0)$ and not with E_{HS}, as done in (2.8). This will generate a new estimate $v_1(r)$ of the interaction and it is clear that the procedure can be iterated by computation of the "exact" $g_1(r)$. In this way we obtain, at the ith iteration,[4]

$$\begin{aligned} \beta v_i(r)=&\beta v_{i-1}(r)+g(r)-g_{i-1}(r) \\ &+\ln[g(r)/g_{i-1}(r)] \\ &+(2\pi)^{-3}\rho^{-1}\int d^3q\, e^{-i\mathbf{q}\cdot\mathbf{r}}[S^{-1}(q)-S_{i-1}^{-1}(q)]\ , \end{aligned} \tag{3.2}$$

where we have used (2.4). Since simulation gives $g_i(r)$ only up to a finite distance, use of (3.2) requires a suitable extension of $g_i(r)$ at large distance like (2.10) in order to obtain $S_i(q)$ without cutoff errors. The iteration will stop when both $g_i(r)-g(r)$ and $S_i(q)-S(q)$ are below a set standard of error which must take into account the precision of the starting $g(r)$ and $S(q)$ and the statistical error of $g_i(r)$ and $S_i(q)$.

It is clear that many variants on this basic scheme can be considered. For instance, Schommers, who first applied a similar approach,[7] considered the function $y_i(r)=g_i(r)\exp[\beta v_i(r)]$. Assuming that one could neglect the change of $y(r)$ when the potential is changed, he used as predictor

$$\beta v_i(r)=\beta v_{i-1}(r)+\ln[g(r)/g_{i-1}(r)]\ , \tag{3.3}$$

with the initial condition

$$\beta v_0(r)=-\ln[g(r)]\ . \tag{3.4}$$

Another predictor[4] derives from a random-phase approximation (RPA) in which the variation of the direct correlation function is equal to the variation of the pair interaction multiplied by β. This gives

$$\begin{aligned} \beta v_i(r)=&\beta v_{i-1}(r) \\ &+(2\pi)^{-3}\rho^{-1}\int d^3q\, e^{-i\mathbf{q}\cdot\mathbf{r}}[S^{-1}(q)-S_{i-1}^{-1}(q)]\ . \end{aligned} \tag{3.5}$$

It is easy to obtain the predictors corresponding to other approximations, for instance, the crossover MHNC equation.[18]

Notice that both (3.3) and (3.5) can be obtained from (3.2) by dropping some of its terms. From what is known in the direct problem we expect that the predictor (3.2) should be very good at short distance in the core region due to the "universality" of the bridge function.[3] It should be less accurate at larger distance where the RPA function (3.5) should be better. Therefore, one could even consider[5] performing some iterations with the predictor (3.2) and some with (3.5). Less clear is what to expect

from Schommers's predictor (3.3), since only at low density the function $y(r)$ becomes really weakly dependent on $v(r)$. The use of the crossover MHNC equation[18] as predictor seems to also be indicated because it should have both the advantages of MHNC and of RPA.

With this kind of approach to inversion it is important that both the starting point $v_0(r)$ and the predictor are as good as possible in order to have fast convergence. This is because at each iteration cycle there is one simulation so that an intrinsic noise is introduced. In this respect, an important difference between the predictors (3.3) and (3.5) compared with (3.2) is that (3.2) contains a direct comparison of $g_i(r)$ and $S_i(q)$ with $g(r)$ and $S(q)$. With (3.3) only $g_i(r)$ and $g(r)$ enter and with (3.5) only the structure factors. In a strict mathematical sense this should not make any difference at convergence because one function is the Fourier transform of the other. But this is not so when we take into account the noise in $g_i(r)$. For instance, on the basis of (3.3) one could be led to believe to have reached convergence because $g(r)-g_i(r)$ is below this statistical noise. However, if the deviations $g(r)-g_i(r)$ are small but not of random character, the difference $S(q)-S_i(q)$ can be significant in some range of q and on the basis of (3.2) one should continue the iteration. In Sec. IV we will present an example of this.

IV. INVERSION FOR THE LENNARD-JONES FLUID

We have first tested the iterative predictor-corrector method with the MHNC predictor in the case of the LJ potential (2.9), a prototype of a simple dielectric fluid, in the triple-point region. The RDF of the molecular-dynamics run with cutoff at 4σ, extended to large distance with the algorithm (2.10), and the related $S(q)$ were used as the input structural data from which the interaction is extracted. As starting potential $v_0(r)$ we use (2.8) with the hard-sphere bridge function $E_{\rm HS}$ corresponding to the Verlet-Weis parametrization[16] of $g_{\rm HS}(r)$ extended inside the core by Henderson and Grundke[19] and the packing fraction is determined by the Lado criterion (2.7). We stress that all this does not require any *a priori* knowledge of the pair interaction which we want to extract.

Starting from this $v_0(r)$ we have performed twelve iterations using (3.2) and we plot some of the results for βv in Fig. 4. For the first five iterations $g_i(r)$ have been computed by Monte Carlo simulations of 10^6 configurations for a system of 864 particles with a cutoff $r_c=3\sigma$. Already at the first iteration the spurious structure at $r\sim 1.7\sigma$ contained in $v_{\rm MHNC}=v_0$ is eliminated and the position of the minimum is given with high precision. However, the value of $v(r)$ at the minimum takes longer to converge but at the fifth iteration (also shown in Fig. 4) the computation could be considered as converged. In fact, the differences $g_5(r)-g_4(r)$ and $S_5(q)-S_4(q)$ were below the level of statistical noise. It can be seen in Fig. 4 that $\beta v_5(r)$ deviates from $\beta v_{\rm LJ}(r)$ in the attractive region rather uniformly by ~ 0.05. In order to understand the origin of this small deviation, starting from $v_5(r)$ we have performed seven additional iterations using as the cutoff the same value $r_c=4\sigma$ of the input computation. Runs of

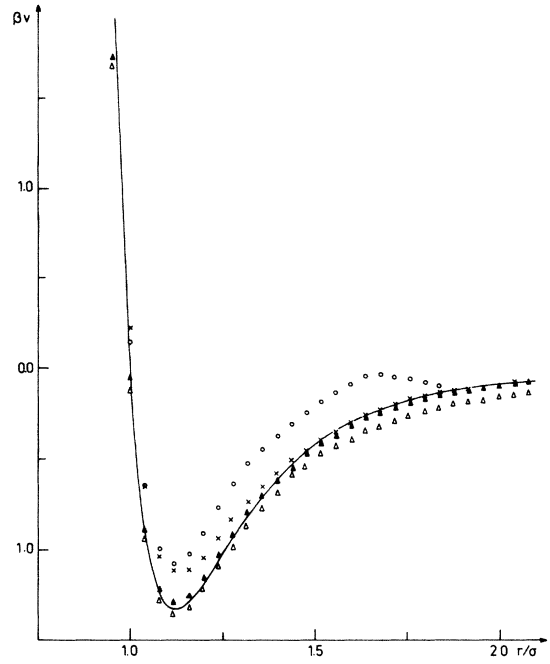

FIG. 4. Test of the iterative predictor-corrector scheme (3.2) for a Lennard-Jones system near triple point ($\rho^*=0.84$, $T^*=0.75$). The initial potential (open circles) is obtained from the MHNC equation (2.8). Crosses and triangles represent the potentials extracted after the first and the fifth iteration, respectively. The solid triangles represent the average of the potentials obtained from iterations 8–12 and the solid line the exact Lennard-Jones potential.

10^6 configurations have been performed with the last two of 2×10^6. The last five iterations give $v_i(r)$ which oscillates around the *correct* answer $v_{\rm LJ}$ by $\sim\pm 0.1$ and the relative $g_i(r)$ differs by less than the statistical noise. It should be noticed that an increase of the value of r_c with simulations of the same number of configurations has the effect of increasing the fluctuation in βv_i. This is a consequence of an increase in the fluctuation of $S(q)$ at small q, which is strongly amplified because $S_i^{-1}(q)$ enters the predictor (3.2). Thus, within this noise level the computation could be considered as converged and in order to improve the statistics we have taken the average of the last five iterations as the final prediction of the potential. In the range $1<r/\sigma<2$ the typical deviation of this average from $\beta v_{\rm LJ}$ is ~ 0.02 and in the core region the deviation is below 3%. For $r/\sigma>2.5$, where $|\beta v_{\rm LJ}|$ is below 0.02, the extracted potential shows some small oscillations around zero, it has a maximum of 0.019 at $r/\sigma=2.72$ and a minimum of -0.012 at $r/\sigma=3.56$. In addition, the positions of these extrema fluctuate widely (up to $\sim 15\%$) from one iteration to the next even for the last ones. It is clear that these small structures are an effect of the statistical noise of our simulation runs. From a practical point of view it would have been better to use longer runs and a smaller number of iterations. However, in this test computation we wanted to check also if the method has some problem of instability due to the noise. Our

computations show that no such problem arises.

As a further test of the method we have considered the same LJ system at $\rho\sigma^3=0.65$ and $k_BT/\varepsilon=1.036$. Now βv_{MHNC} is rather good (see Fig. 3) and after four iterations $v_{\mathrm{LJ}}(r)$ is reproduced with very high precision. At such a smaller density the value of the cutoff is less crucial and in these computations we have used $r_c=2.5\sigma$.

The Schommers's scheme (3.3) is attractive because it is easier to use, not requiring the extension of $g(r)$ at large distances. For this reason we have tested this method under the same conditions. For the triple-point state we have considered the computation as apparently converged after 13 iterations, starting from the initial potential (3.4). In fact, the $g_i(r)$'s of the last few iterations and the initial $g(r)$ differ by less than the statistical noise (see Fig. 5). However, the extracted potential (Fig. 6) differs greatly from v_{LJ}.

The data shown in Figs. 5 and 6 illustrate very well the difficulty encountered in the inversion under triple-point conditions. Two radically different potentials like v_{LJ} and v_{13} (cf. Fig. 6) give a RDF which differs everywhere by less than 0.01. This is the screening of the weak features of the potential by its hard part. However, it can be noticed from Fig. 5 that the difference between these two RDF has a systematic dependence on r. This gives rise in the corresponding structure factors to deviations well above the noise level. As a comparison in Fig. 5 we give also the difference between the $g(r)$ of the LJ system and

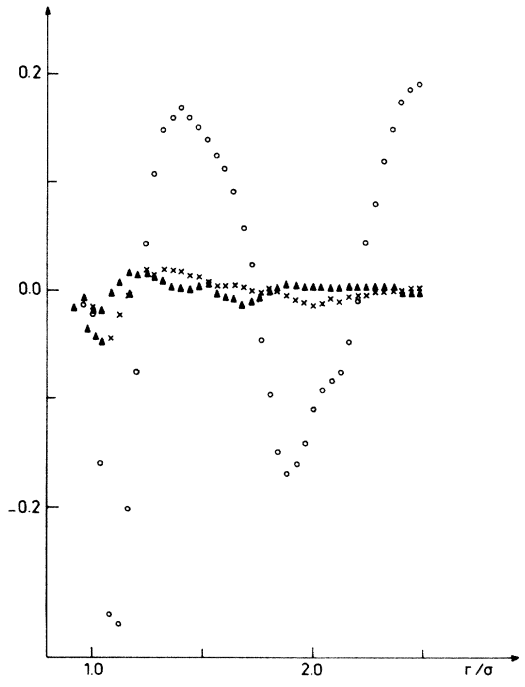

FIG. 5. Test of Schommers's iterative inversion scheme [Eq. (3.3)] for a Lennard-Jones system near triple point ($\rho^*=0.84$, $T^*=0.75$). Open circles, difference between the RDF's corresponding to the Lennard-Jones potential (g_{LJ}) and the initial potential βv_0 [Eq. (3.4)]; crosses, difference between g_{LJ} and g_{13}, RDF at the 13th iteration; solid triangles, difference between g_{LJ} and the RDF of iteration 12 in our scheme.

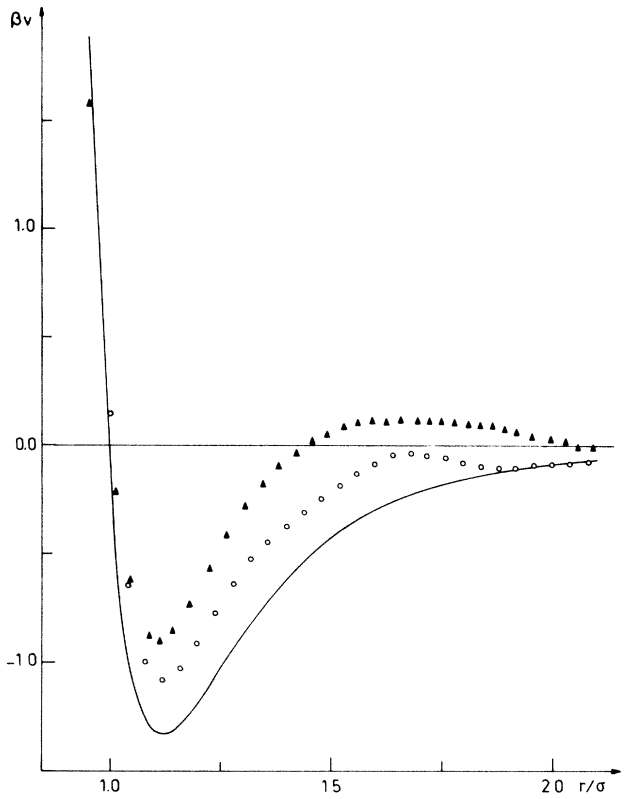

FIG. 6. Test of Schommers's inversion scheme [Eq. (3.3)] for a Lennard-Jones system near triple point ($\rho^*=0.84$, $T^*=0.75$). The solid triangles represent the potential βv_{13} extracted at the 13th iteration, the open circles the potential obtained from the MHNC equation (2.8), and the solid line the Lennard-Jones potential.

the RDF corresponding to convergence of our scheme as discussed above. This deviation is very small but also of a more random nature.

The initial estimate (3.4) for $\beta v_0(r)$ is much worse than the MHNC one and one could suspect that the poor performance of Schommers's scheme is due to such a bad starting point. Now there is no reason for not using, for instance, βv_{MHNC} as the initial potential also in Schommers's iterative loop (3.3). We have performed this computation for the LJ system at the intermediate density $\rho\sigma^3=0.65$. βv_{MHNC} is rather close to the correct answer (see Fig. 4) and we have performed six iterations with simulations of 10^6 configurations. The v_i so obtained do not show a global improvement with respect to the starting v_{MHNC}; in some regions of r, v_i becomes closer to v_{LJ} but in other regions v_i moves away from v_{LJ}. We cannot say if much longer simulation runs could resolve this difficulty but it is clear that this scheme is, at the least, impractical and can lead to an apparent convergence to a wrong answer.

V. INVERSION FOR A MODEL ALUMINUM POTENTIAL

The second test of our inversion procedure has been for the model Al potential[17] already described in Sec. II. The

procedure follows exactly the same pattern as in the case of the LJ fluid. The starting $g(r)$ considered as "exact" is obtained from a Monte Carlo simulation of 7×10^6 configurations and extended from $r_c=2.04r_0$, where $r_0=4.234$ Å is the size of the Wigner-Seitz cell. Starting from $v_0=v_{\mathrm{MHNC}}$ with η given by (2.7) we have performed eight iterations with (3.2) and $g_i(r)$ are computed with simulations each of 4×10^6 configurations with the same cutoff $r_c=2.04r_0$. Already $v_1(r)$ (see Fig. 7) reproduces with good precision the positions of the extrema and these remain very stable during the subsequent iterations. As in the case of the LJ potential, the convergence of the values of $v(r)$ at the extrema is slower and this is in part due to the effect of statistical noise. However, already at the fourth iteration one has a reasonably accurate estimate of v_{Al} and at the eighth iteration there is almost no change in $g(r)$, so that the computation was considered as converged. Table III shows that the agreement between βv_8 and βv_{Al} is very good everywhere, the deviations being typically of order ±0.02 and of order of 5% in the core region. From results of simulations of different lengths which we have performed it is clear that this residual error could be reduced still further by longer simulations.

The oscillations of v_{Al} in the tail region have a very small amplitude, for instance, $\beta v_{\mathrm{Al}}=-0.03$ and 0.02 at the two last extrema before $r=2r_0$. Therefore, the extracted interaction reproduces the amplitude of these structures with only modest relative precision. We want to stress, however, that our inversion procedure leaves no doubt about the existence of these structures. In fact, in all iterations one finds these weak structures almost at the same positions, the variation in these positions being less than 3%. This behavior can be contrasted with the one found for the weak and spurious structures for $r/\sigma>2.5$ in the case of the extracted potential for the LJ system. In that case, not only do the values of βv_i at these extrema fluctuate but also their positions have very large fluctuations. In this way one can very well discriminate genuine weak structures from spurious ones. On the other hand, if one needs to know with high precision the amplitude of these weak structures, simulations longer than the ones we have performed are needed.

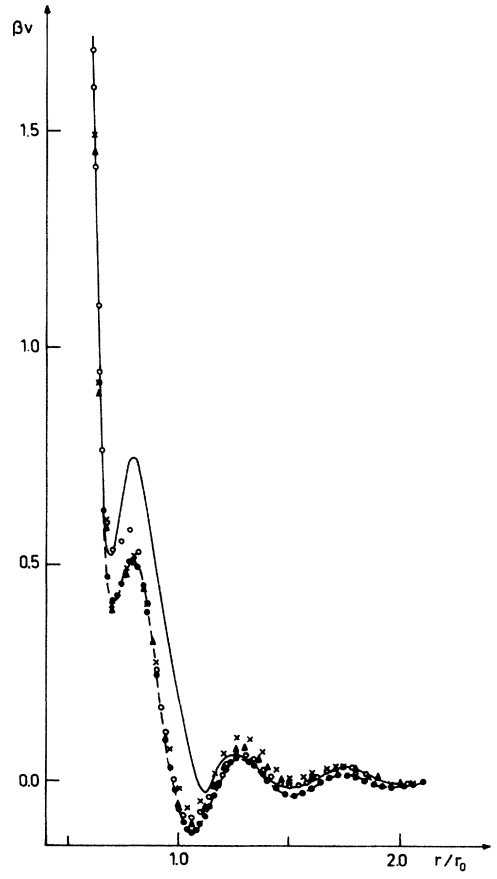

FIG. 7. Inversion procedure (3.2) applied to an aluminumlike model. The solid line is the potential βv_{MHNC} obtained from the MHNC equation (2.8) (input). The open circles and the crosses represent the potentials extracted at the first and fifth iteration, respectively, the triangles the average potential of iterations 4–8, the solid circles and dashed line the model aluminum potential.

VI. INVERSION OF EXPERIMENTAL DATA WITH THE ITERATIVE PREDICTOR-CORRECTOR METHOD

The application of our inversion scheme to experimental data raises many questions which we try to answer in this section. First is the question of many-body forces present in a real fluid but absent in the models tested in the previous sections. It is clear that in the case of inversion of experimental data the three-and-more–body interactions will be replaced by an effective two-body interaction added to the genuine one. We do not expect that this will give any serious problem of convergence to our method. In fact, we have already a test of this[5] in the case of a quantum Bose fluid. In that case, the formally identical problem[4] is to find the Jastrow function, which has the role of $\exp[\beta v(r)]$ in the present case, which reproduces a given RDF $g(r)$ corresponding to the ground state Ψ_0 of the system. This $g(r)$ was obtained from the Green-function Monte Carlo method,[20] which gives an *exact* sampling of this ground state. This Ψ_0 contains implicitly correlations between more than two particles and, in particular, it is well established[21] that triplet correlations in Ψ_0, the equivalent of a triplet interaction in the classical case, are very important. The inversion method we are using here had no difficulty of convergence in that case.

The second problem arises from the long-range tail of $v(r)$ beyond the cutoff r_c, which one must necessarily use in a simulation. An estimate of the effect of the long-range tail of $v(r)$ on the short-range part of the RDF $g(r)$ can be obtained by comparing the runs with cutoff 4σ and 2.5σ performed for the LJ fluid (cf. Sec. II). The difference between the $g(r)$ with cutoff 4σ and the two $g(r)$'s with cutoff 2.5σ is within the statistical error on these $g(r)$'s. We further have studied the effect of the tail of the LJ potential under triple-point conditions when $r_c=4\sigma$ by computing $g(r)$ by solving a MHNC equation obtained from (2.6) by replacing $E(r/v_{\mathrm{LJ}})$ of the untruncated potential with the one of the truncated potential.

This bridge function is obtained from a formula similar to (3.1) by using the simulation result for $g(r)$. The effect on $g(r)$ is extremely small so that the error introduced in the extracted potential at *short* distance by the neglect of the tail of $v(r)$ is completely negligible. On the other hand, if scattering data of extremely high precision at very small q were available, this information could be used to obtain information on the tail of $v(r)$ beyond the cutoff r_c even with our method. In this case, the predictor based on the crossover MHNC (Ref. 18) should be used due to the built-in RPA approximation, which is expected to be very accurate for a long-range tail. The iteration procedure does not modify the extracted interaction beyond r_c.

The finite size of the system in the simulation affects our inversion procedure in two ways. First, because it gives $g(r)$ only up to a finite range and one has to extend $g(r)$ at larger distances. Since the extension algorithm (2.10) is only approximate, this introduces an error in the extracted potential. We have shown in Sec. II that for commonly used values of r_c ($r_c \sim 2.5\sigma$—4.0σ) the residual error is rather small. On the other hand, if the quality of the input data is so high as to warrant this, one could use a better extension scheme.[22]

The second effect of finite size is due to the N dependence of $g(r)$. For the large systems which we use the dominant contribution is the N^{-1} term, which is known to have the form[23]

$$g(r)=g_N(r)+\frac{1}{N}\Delta g(r) , \tag{6.1}$$

$$\Delta g(r)=\tfrac{1}{2}S(0)\frac{\partial^2 g(r)}{\partial\rho^2} , \tag{6.2}$$

where $g(r)$ is the RDF of the infinite system, N is the number of particles, and $S(0)=\rho k_B T k_T$ is the reduced isothermal compressibility. In (6.2), $g(r)$ and $S(0)$ can be either the quantities for the infinite system or those of the finite one. In the computations of Secs. IV and V, we did not have to worry about this $1/N$ effect because both the starting $g(r)$ and those obtained with the iterations are similarly affected and in this way no bias is introduced in the extracted potential. This is no longer true when the starting $g(r)$ derives from experiment and our inversion procedure will interpret the absence of this $1/N$ contribution in the experimental data by a suitable modification in the extracted potential. There are different ways in which one can correct this error and the following is one. It has already been shown[22] that the MHNC equation can be used to compute $\Delta g(r)$ as defined by (6.2) by solving that equation at neighboring densities with the hard-sphere bridge function at a packing fraction determined at each density by (2.8). Suppose that with our predictor-corrector method we have extracted an interaction which we call $v_N(r)$ because it is affected by the finite-size effect. Using this $v_N(r)$ we can now compute $\Delta g(r)$ with $S(0)$ and $\partial^2 g(r)/\partial\rho^2$ given by MHNC as explained above. Notice that for this purpose $\partial^2 g(r)/\partial\rho^2$ must be computed keeping $v_N(r)$ fixed even if in the real system the pair interaction is density dependent. If we now approximate the bridge function corresponding to the unknown $v(r)$ with the one of a hypothetical *infinite* system interacting with $v_N(r)$ we find

$$\beta v(r)=\beta v_N(r)+g(r/v)-g(r/v_N)-c(r/v)+c(r/v_N)-\ln\left[\frac{g(r/v)}{g(r/v_N)}\right] , \tag{6.3}$$

and using (6.1) for $g(r,v_N)$ and the fact that $g(r/v)=g_N(r/v_N)$ we finally have

$$\beta v(r)=\beta v_N(r)-(1/N)\Delta g(r/v_N)+(1/N)\Delta c(r/v_N)+\ln\left[1+\frac{1}{N}\frac{\Delta g(r/v_N)}{g(r/v_N)}\right] . \tag{6.4}$$

Here, $(1/N)\Delta c(r/v_N)$ is the $1/N$ correction term corresponding to the $(1/N)\Delta g(r)$ variation of the RDF as given by the OZ relation. Equation (6.4) is correct to order $1/N$ and the only significant approximation is the computation of $\Delta g(r/v_N)$ with MHNC.

The final point concerns the step size Δr used in simulation. Simulation in reality gives a histogram for the RDF and Δr is chosen to be not too small, typically $\Delta r/\sigma \sim 0.01$—$0.02$, in order to have sufficient statistics. In the core region $g(r)$ has a strong curvature so that the average of $g(r)$ over Δr is rather different from the value of $g(r)$ at the mean position. On the contrary, no such problem is present in $g(r)$ deduced from the experimental data. One can take care of this problem by taking the average of $g(r)$ deduced from the experimental data over the step size used in simulation. The other possibility, which is preferable, is to obtain from simulation directly a sampling of $y(r)=e^{\beta v(r)}g(r)$ because this function is smooth also in the core region.

VII. INVERSION OF EXPERIMENTAL STRUCTURAL DATA FOR Na

In this section we present the results of the application of our inversion scheme to Na at temperature $T=100\,^{\circ}\mathrm{C}$ and density 0.929 g/cm^3. For this thermodynamic state an experimental structure factor $S(q)$ is available[24] in the domain of wave vectors q from 0 to 8.9 Å^{-1}. This domain, unfortunately, does not extend to sufficiently high values of q in order to obtain the two-body pair distribution function $g(r)$ by direct Fourier transform of the experimental structure factor $S_{\mathrm{expt}}(q)$. In fact, when Fourier transforming the experimental structure factor we obtain a correlation function $g_0(r)$, which is nonzero and oscillates in the range of distances 0—2.7 Å corresponding to the range where the interaction of two sodium atoms is strongly repulsive. In order to correct this defect of $g_0(r)$ we extrapolated $S_{\mathrm{expt}}(q)$ for values of q larger than 8.9 Å^{-1} in the following way. We first force $g_0(r)$ to be zero between $r=0$ and $0.75r_M$, where r_M corresponds to the position of the main peak of $g_0(r)$. We take the Fourier transform of this new function $g_0'(r)$ for q vectors varying from 0 to 80 Å^{-1} and obtain a function $S_0'(q)$ which differs obviously from $S_{\mathrm{expt}}(q)$ in the domain 0—8.9 Å^{-1}. We then construct a function $S_1(q)$ by substituting the experimental values for $0<q<8.9$ Å^{-1} into $S_0'(q)$ and calculate a new RDF $g_1(r)$. The function $g_1(r)$ has still some spurious oscillations for small values of r and we re-

peat the preceding procedure until a function $g(r)$ is obtained which is reasonably close to zero for $r<0.75r_M$ [$|g(r)|\sim 0.005$]. When $g(r)$ is now taken as zero in this interval, its Fourier transform is in good agreement with $S_{\text{expt}}(q)$ for $q\leq 8.9$ Å^{-1}. For low k values ($k<0.3$ Å^{-1}) the difference between $S_{\text{expt}}(q)$ and the $S(q)$ obtained by Fourier transform of $g_{\text{expt}}(r)$ is less than 0.001; for $0.3<k<0.7$ Å^{-1} the difference is smaller than 0.01, the maximum discrepancy occurs for $0.7<k<1.5$ Å^{-1}, where it is of the order ~ 0.03 with a maximum of 0.044 at $k=1.2$ Å^{-1}. For $k>1.5$ Å^{-1}, the difference is always smaller than 0.016. One also can notice that for $k>6$ Å^{-1}, the error on the experimental values is quite large. It is worth noticing that in the iteration process just described the values of $g(r)$ for $r>0.85r_M$ are very stable, for instance, the value of $g(r)$ at r_M is modified by less than 0.5%.

In order to obtain a first estimate of the potential from the MHNC equation (2.8), we need not only $g(r)$ but also $c(r)$. The direct correlation function has been calculated from (2.4) using for $S(q)$ the final result of the iteration process [i.e., $S(q)=S_{\text{expt}}(q)$ for $0<q<8.9$ Å^{-1} and is extrapolated for $q>8.9$ Å^{-1}]. This $c(r)$ is not completely consistent via the OZ relation with a $g(r)$, which vanishes at short distances. This introduces an intrinsic limit to how well our iterative procedure can converge and we estimate that this limit is $\Delta g\leq 0.10$–0.15 for $0.7r_M\leq r<0.85r_M$ corresponding to the range of r, where $g_{\text{expt}}(r)$ is corrected by the extension procedure of $S(k)$.

We stress that the extension procedure is needed for the reason that, $S_{\text{expt}}(q)$ being known only in a limited domain of q vectors with an error of 0.5–1.0%, a precise estimate of $g(r)$ is precluded for small r and, consequently, the determination of the repulsive part of the effective two-body interaction potential is made difficult.

The potential βv_0 obtained from the MHNC relation (2.8) is shown in Fig. 8; it is determined using the Verlet-Weis bridge function $E_{\text{HS}}(r,\eta)$ at $\eta=0.47$ corresponding to a hard-sphere diameter of 3.33 Å. Starting from this potential we have performed five iterations following the scheme summarized by relation (3.2). The Monte Carlo simulations were preformed with a system of $N=864$ particles interacting by the potentials βv_i ($i=0,1,\ldots,5$) truncated at 8.7 Å and for each simulation 10^6 configurations were generated.

After the second iteration the potentials found by inversion are very similar. As discussed for the LJ and Al cases the differences between the potentials subsequent to the second iteration are mainly due to the statistical uncertainties on the simulated correlation functions. Figure 8 shows the potentials βv_4 and βv_6 together with potential $\beta\bar{v}_{2-6}$ (average of $\beta v_2,\beta v_3,\ldots,\beta v_6$). This last potential crosses zero at $r=3.3$ Å, has two minima at $r\sim 3.9$ and 7.44 Å corresponding to -456 and -38 K and a maximum at 5.76 Å of value -5 K. The mean-square deviation of $\bar{v}_{2-6}$ varies between ± 25 K at the first minimum and ± 12 K at the second minimum. The potential $\beta\bar{v}_{2-6}$ is very similar to the interaction used by Lee *et al.*[25] in a numerical simulation of Na. This interaction potential has two minima at ~ 3.9 and 7.3 Å with values ~ -475 and -20 K, respectively, and a maximum at 5.6 Å with

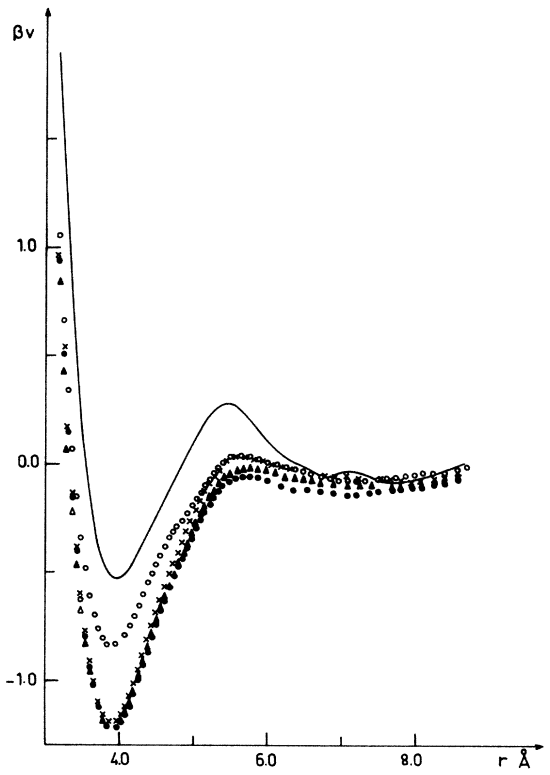

FIG. 8. Inversion procedure (3.2) applied to the experimental structure factor of Na at 100 °C. The solid line represents the input potential obtained from the MHNC equation (2.8); the open circles, crosses, and solid circles the potentials extracted after 1, 4, and 6 iterations, respectively, the triangles the average potential for iterations 2–6.

value ~ 50 K; when used in a molecular-dynamics simulation, it gives a correlation function $g(r)$ in good agreement with the experimental $g(r)$. Our potential is also in qualitative agreement with the potential used by Murphy and Klein[26] in a numerical simulation of Na; this potential has minima located at 3.82 and 7.43 Å with values -356 and -11 K and a maximum at 5.6 Å with value 50 K. Gonzales and Torra[27] have done a systematic study of five different potentials for Na by molecular-dynamics simulation. These potentials are rather different from the potential found in our inversion scheme. In fact, we remark that the heights of the main peak of $g(r)$ calculated from these five potentials differ by 5% from the experimental one.

From Table IV, it is seen that the simulated pair correlation functions corresponding to the potentials $\beta v_0,\beta v_1,\ldots,\beta v_5$ and $\bar{g}(r)$, average value of the $g(r)$'s of the three last simulations, are in agreement with the experimental $g(r)$, taking into account the inconsistency between $h-c$ and g_{expt} for small r.

We conclude that the inversion scheme applied to experimental structure factor seems to be a convergent procedure and able to give a good estimate of the effective two-body interactions in liquid metals. However, we recall that in the present calculations for Na the potential

depends for distance $r > 3$ Å on the correlation procedure described above, which is necessary for obtaining acceptable values for the experimental $g(r)$ for $r < 3$ Å. This uncertainty is due to the fact that experimental values of $S_{\text{expt}}(q)$ at large q are missing and could obviously be removed if these experimental values were known. In view of this uncertainty we have not pushed the iteration procedure to the same level of convergence as in the case of

TABLE IV. $g(r)$ functions from $\beta v_0, \beta v_1, \ldots, \beta v_5$ potentials for Na at 100 °C and $\rho = 0.949$ g/cm^3, $\bar{g}_{3-5}(r)$ is the average of $g_3(r)$, $g_4(r)$, and $g_5(r)$. $g_{\text{expt}}(r)$ is obtained from $S_{\text{expt}}(q)$ following the procedure described in Sec. VII ($\sigma = 3.0$ Å).

r/σ	$g_0(r)$	$g_1(r)$	$g_2(r)$	$g_3(r)$	$g_4(r)$	$g_5(r)$	$\bar{g}_{3-5}(r)$	$g_{\text{expt}}(r)$
0.92	0.001	0.001	0.001	0.001	0.000	0.000	0.001	0.000
0.94	0.006	0.009	0.007	0.010	0.008	0.010	0.009	0.007
0.96	0.017	0.022	0.015	0.022	0.016	0.020	0.018	0.016
0.98	0.048	0.056	0.038	0.051	0.041	0.045	0.044	0.033
1.00	0.143	0.185	0.140	0.183	0.151	0.171	0.161	0.147
1.02	0.313	0.404	0.324	0.399	0.334	0.375	0.358	0.320
1.04	0.536	0.665	0.546	0.653	0.560	0.615	0.593	0.545
1.06	0.794	0.955	0.809	0.942	0.829	0.897	0.869	0.809
1.08	1.077	1.259	1.100	1.240	1.119	1.194	1.164	1.098
1.10	1.360	1.552	1.399	1.533	1.420	1.494	1.462	1.392
1.12	1.627	1.815	1.689	1.794	1.709	1.772	1.741	1.672
1.14	1.887	2.038	1.948	2.017	1.961	2.015	1.985	1.924
1.16	2.121	2.206	2.170	2.190	2.167	2.212	2.185	2.132
1.18	2.310	2.325	2.344	2.307	2.331	2.346	2.332	2.288
1.20	2.437	2.395	2.444	2.379	2.439	2.420	2.420	2.390
1.22	2.506	2.405	2.493	2.391	2.485	2.442	2.453	2.432
1.24	2.523	2.364	2.487	2.349	2.470	2.415	2.430	2.426
1.26	2.473	2.282	2.420	2.271	2.409	2.340	2.360	2.369
1.28	2.370	2.170	2.318	2.169	2.308	2.225	2.255	2.276
1.30	2.229	2.040	2.185	2.045	2.173	2.093	2.124	2.153
1.32	2.069	1.896	2.031	1.900	2.019	1.944	1.974	2.010
1.34	1.898	1.742	1.870	1.756	1.854	1.781	1.816	1.856
1.36	1.723	1.587	1.704	1.611	1.689	1.624	1.657	1.698
1.38	1.558	1.441	1.543	1.468	1.529	1.469	1.502	1.543
1.40	1.404	1.306	1.392	1.337	1.374	1.327	1.357	1.397
1.42	1.265	1.187	1.247	1.210	1.239	1.203	1.225	1.261
1.44	1.139	1.080	1.123	1.099	1.122	1.087	1.108	1.141
1.46	1.029	0.984	1.020	1.006	1.014	0.986	1.006	1.036
1.50	0.861	0.842	0.844	0.859	0.844	0.837	0.846	0.870
1.54	0.739	0.746	0.720	0.758	0.728	0.731	0.734	0.755
1.58	0.651	0.678	0.638	0.691	0.644	0.665	0.660	0.677
1.62	0.581	0.634	0.587	0.641	0.584	0.619	0.608	0.623
1.66	0.534	0.601	0.547	0.610	0.549	0.580	0.572	0.585
1.70	0.502	0.584	0.526	0.589	0.530	0.563	0.552	0.564
1.74	0.493	0.582	0.522	0.583	0.528	0.559	0.548	0.560
1.78	0.507	0.591	0.541	0.591	0.544	0.573	0.562	0.573
1.82	0.543	0.619	0.573	0.619	0.582	0.603	0.594	0.604
1.86	0.603	0.662	0.628	0.662	0.633	0.654	0.644	0.652
1.90	0.680	0.727	0.699	0.720	0.707	0.719	0.711	0.717
1.94	0.776	0.800	0.790	0.793	0.795	0.804	0.796	0.796
1.98	0.891	0.882	0.894	0.874	0.893	0.892	0.888	0.882
2.02	1.007	0.969	0.992	0.956	0.997	0.979	0.981	0.969
2.06	1.106	1.051	1.090	1.036	1.084	1.068	1.069	1.050
2.10	1.188	1.125	1.166	1.107	1.162	1.142	1.144	1.119
2.14	1.243	1.192	1.220	1.175	1.218	1.204	1.204	1.175
2.18	1.279	1.241	1.261	1.222	1.260	1.248	1.248	1.218
2.22	1.311	1.274	1.287	1.261	1.286	1.280	1.278	1.250
2.26	1.327	1.294	1.291	1.282	1.289	1.293	1.289	1.267
2.30	1.295	1.293	1.282	1.279	1.278	1.293	1.283	1.269
2.34	1.252	1.266	1.263	1.261	1.258	1.265	1.262	1.255
2.38	1.203	1.226	1.230	1.228	1.220	1.227	1.226	1.227
2.42	1.160	1.177	1.181	1.180	1.180	1.176	1.179	1.186
2.46	1.119	1.119	1.130	1.130	1.131	1.118	1.127	1.138
2.50	1.077	1.063	1.076	1.075	1.078	1.054	1.071	1.084

the model systems considered in the previous sections. The trend of the successive $v_i(r)$ is similar to that found for the model systems and this leaves no doubt that the same level of convergence could be obtained if longer computations had been done. For the same reason we have not computed the $1/N$ correction term given by (6.4). We also remark that the published experimental values of $S_{\text{expt}}(q)$ for Na at $T=100\,^{\circ}\text{C}$ (Refs. 24 and 28) and higher temperatures[24,29] differ noticeably, so that use of experimental data different from Ref. 24 would have led to a potential different from the one given in Fig. 8. In view of the uncertainty in presently available data, we stress the fact that the Na potential calculated in this work is consistent with the data of Ref. 24, but not necessarily with all published data for structure factors of Na.

VIII. DISCUSSION

The main result of the present study is that the inversion scheme for static structure factors summarized by Eqs. (3.1) and (3.2) is a reliable one and allows a precise determination of effective two-body potentials up to triple-point conditions. Two lessons have been drawn. First, because experimental structure factors for liquid metals, in particular Na, are generally measured accurately in a limited domain of q vectors and low q values are sometimes missing, both the determination of the short-range repulsive part of the potential and that of the long-range part are problematic. These difficulties are obviously also present in inversion schemes[14] which use as input directly the experimental structure factor but not also the corresponding pair correlation function as in the present case. The second lesson concerns the convergence of the iterative inversion scheme. Convergence of the method does not depend in a crucial way on the initial estimate $v_0(r)$ of the potential as due, for instance, on the choice of the value of the hard-sphere diameter in the bridge function or on the use of the PY approximation for the bridge function in place of a more accurate one. However, the method might not converge if $v_0(r)$, which initiates the iterative process, is too far from the correct result. This last point was the reason why we were unable to apply our inversion scheme to the experimental structural data[29] for Na at 550 °C. For this thermodynamic state the evaluation of the initial potential v_{MHNC} was poor [due to a very imprecise determination of $c(r)$ from the experimental data also due to lack of data for $q<0.5$ Å] and the corresponding simulated pair correlation function too far from the experimental $g(r)$ to obtain convergence of the iterative process. However, we have verified that potential βv_6 (drawn on Fig. 8), when used in a MC simulation of $g(r)$ at 550 °C gives results in excellent agreement with the experimental $g(r)$ outside the core region for $r>3$ Å. For instance, the positions and heights of the two first maxima of the experimental $g_{\text{expt}}(r)$ and calculated $g_{\text{MC}}(r)$ are, respectively, $g_{\text{expt}}(3.63\text{ Å})=1.87$, $g_{\text{MC}}(3.63\text{ Å})=1.87$, and $g_{\text{expt}}(6.90\text{ Å})=1.15$, $g_{\text{MC}}(6.96\text{ Å})=1.14$, and those of the two first minima are $g_{\text{expt}}(5.16\text{ Å})=0.76$, $g_{\text{MC}}(5.25\text{ Å})=0.73$, and $g_{\text{expt}}(8.40\text{ Å})=0.93$, $g_{\text{MC}}(8.52\text{ Å})=0.92$. This result shows that the potential found by inversion of the data at 100 °C also reproduces the experimental data at 550 °C. Comparison of the MC and experimental $g(r)$'s for $r<3$ Å is not significant due to the imprecise determination of both the repulsive part of the potential and of $g_{\text{expt}}(r)$ at 550 °C in this domain.

Finally, the inversion scheme is readily successful for thermodynamic states away from the triple point. Under triple-point conditions the method is also successful provided that experimental data are sufficiently accurate and known on a wide range of wave vectors so that a reliable $g(r)$ can be deduced.

We have inverted the scattering data of Na at 100 °C as a test of our method. The necessity of a significant extension of the data at large q and the presence of substantial deviations between these data and those of other measurements suggests that it is too premature to make a detailed comparison between the extracted potential and the results of theoretical computations.

ACKNOWLEDGMENTS

One of us (L.R.) acknowledges financial support from the Ministero dell Pubblica Istruzione (Italy) and the Gruppo Nazionale di Struttura della Materia (Italy). Laboratoire de Physique Théorique et Hautes Energies is a Laboratoire associé au Centre National de la Recherche Scientifique.

[1]See, for instance, J. P. Hansen and I. R. McDonald, *Theory of Simple Liquids* (Academic, New York, 1976).
[2]M. D. Johnson, P. Hutchinson, and N. H. March, Proc. R. Soc. London Ser. A **282**, 283 (1964).
[3]Y. Rosenfeld and N. W. Ashcroft, Phys. Rev. A **20**, 1208 (1979).
[4]L. Reatto, Phys. Rev. B **26**, 130 (1982).
[5]G. L. Masserini and L. Reatto, Phys. Rev. B **30**, 5367 (1984).
[6]A preliminary report of some of our computations is contained in D. Levesque, J. J. Weis, and L. Reatto, Phys. Rev. Lett. **54**, 451 (1985).
[7]W. Schommers, Phys. Rev. A **28**, 3599 (1983).
[8]L. Verlet, Phys. Rev. **165**, 201 (1968).
[9]W. G. Madden and S. A. Rice, J. Chem. Phys. **72**, 4208 (1980).
[10]P. Hutchinson and W. R. Conkie, Mol. Phys. **24**, 567 (1972).
[11]M. Brennan, P. Hutchinson, M. J. L. Sangster, and P. Schofield, J. Phys. C **7**, L 411 (1974).
[12]S. K. Mitra, P. Hutchinson, and P. Schofield, Philos. Mag. **34**, 1087 (1976).
[13]F. Lado, Phys. Lett. **89A**, 196 (1982).
[14]M. W. C. Dharma-wardana and G. C. Aers, Phys. Rev. B **28**, 1701 (1983); G. C. Aers and M. W. C. Dharma-wardana, Phys. Rev. A **29**, 2734 (1984).
[15]R. Kumaravadivel (unpublished).
[16]L. Verlet and J. J. Weis, Phys. Rev. A **5**, 939 (1972).
[17]L. Dagens, M. Rasolt, and R. Taylor, Phys. Rev. B **11**, 2726 (1975).
[18]S. M. Foiles, N. W. Ashcroft, and L. Reatto, J. Chem. Phys.

80, 4441 (1984).
[19]D. Henderson and E. W. Grundke, J. Chem. Phys. **63**, 601 (1975).
[20]P. A. Whitlock, D. M. Ceperley, G. V. Chester, and M. H. Kalos, Phys. Rev. B **19**, 5598 (1979).
[21]K. Schmidt, M. H. Kalos, M. A. Lee, and G. V. Chester, Phys. Rev. Lett. **45**, 573 (1980).
[22]S. M. Foiles, N. W. Ashcroft, and L. Reatto, J. Chem. Phys. **81**, 6140 (1984).
[23]J. L. Lebowitz and J. K. Percus, Phys. Rev. **122**, 1675 (1961).
[24]A. J. Greenfield, J. Wellendorf, and N. Wiser, Phys. Rev. A **4**, 1607 (1971).
[25]T. Lee, J. Bisschop, W. Van der Lugt, and W. F. Van Gunsteren, Physica B **93**, 59 (1978).
[26]R. D. Murphy and M. L. Klein, Phys. Rev. A **8**, 2640 (1973).
[27]J. M. Gonzales Miranda and V. Torra, J. Phys. F **13**, 281 (1983).
[28]M. J. Huijben and W. Van der Lugt, Acta Cryst. A **35**, 431 (1979).
[29]Y. Waseda, *The Structure of Noncrystalline Materials* (McGraw-Hill, New York, 1980).